Materials of Controlled Shape and Stiffness with Photocurable Microfluidic Endoskeleton

By *Suk Tai Chang, Ahmet Burak Uçar, Garrett R. Swindlehurst, Robert O. Bradley IV, Frederick J. Renk,* and *Orlin D. Velev**

Microfluidic systems have been the focus of intense research and development as they promise a multitude of advantages in the chemical and biological laboratory practice, such as rapid analysis of samples of small sizes, high resolution and sensitivity, easy automation, and direct integration with sample pretreatment and detection systems on a single chip.[1–5] Microfluidics has already revolutionized some aspects of biosensing and microassays,[6–10] chemical microsynthesis,[4,11–13] and fabrication of special colloidal particles.[14–18] The potential of microfluidics in other areas of technology has only recently begun to be realized and investigated. A few examples of unconventional use of microfluidic technology include fabricating optofluidic devices based on the large refractive-index contrast of liquid/liquid or liquid/air cladding through microchannels,[19–22] performing digital coding/decoding and logic operations by control of streams of droplets and fluorescent molecules,[23–25] design of electronic paper based on electrowetting,[26] and, notably, fabrication of 3D metallic microstructures by solidifying liquid solder into microchannel molds, called ''microsolidics.''[27] One promising, yet largely unexplored, area is the fabrication of materials with embedded microchannel networks, where the flow, pressure, color, and other properties of the liquid inside the channels impart a certain function to the matrix material in which the network is embedded. Microchannels in thin elastomeric polydimethylsiloxane (PDMS) sheets filled with viscous liquid have been used as a means to produce reusable strongly adhesive materials without sticky layers. The large increase in the adhesion forces results from the crack-arresting properties of microchannels and the surface stresses caused by capillary forces.[28,29] Toohey et al. have demonstrated the use of 3D microvascular networks in a self-healing material, which is inspired by the functionality of natural skin derived from its vesicular blood network.[30] Their self-healing composite is capable of multiple healing cycles by capillary wicking of liquid polymerizable epoxy through the cracks, reaching the 3D microvascular network embedded in the substrate.

We describe here a microfluidic material in the form of flexible sheets that can be solidified on demand by light to acquire specific shapes. The matrix of the material is thin sheets of PDMS. The microfluidic-channel networks embedded in the elastomer are filled with liquid photocurable polymer. The materials formed in this way possess the unique ability to ''memorize'' and retain a certain user-defined shape upon illumination. When the microchannel networks are deformed and exposed to UV light, the photoresist inside the channels is solidified and subsequently acts as the endoskeleton within the PDMS layer, locking in the programmed shape. The bending and stretching moduli of the materials with solidified endoskeleton increase drastically. Even if the resulting sculptured sheets are deformed, the ''memorized'' shapes are recovered after the external force causing the deformation is removed.

The procedure for fabrication of shape-controlled microchannel materials is schematically illustrated in Figure 1. The microfluidic channels inside PDMS were fabricated using soft lithography.[31,32] Two PDMS sheets with arrays of channels facing each other in perpendicular directions were sealed irreversibly by air-plasma treatment (Fig. 2). Liquid SU-8 (photocurable epoxy resin) was injected into the microchannel network using a syringe. The filling was done on a hot plate to lower the viscosity and improve the SU-8 wetting of PDMS. The elastomer sheets with microchannel networks filled with liquid SU-8 prepolymer are transparent, soft, and easily bent, similarly to the original silicone rubber (Fig. 3a). The transparent PDMS host can transmit incident light in the near-UV region (350–400 nm), where SU-8 photopolymer is light-sensitive. The soft material filled with liquid SU-8 could be deformed into a variety of shapes, such as wave, spiral, saddle, and pocket, and then solidified by exposure to UV light for 15 min. The resulting PDMS slabs with solidified internal networks after the UV exposure retained the defined deformation, while still having soft and rubber-like surfaces (Fig. 3b–d). The PDMS sheets with photocured network could be stretched, bent, or twisted manually with high recoverable strain.

The SU-8 photoresist has high mechanical stability, which enables its application in reliable replication and reinforcement of sophisticated microstructures.[33–35] The elastic modulus of PDMS is 0.75 MPa[33] and the one of SU-8 after complete crosslinking is 4400 MPa.[33,36] Thus, solidification of the SU-8 prepolymer in the PDMS microchannels should increase drastically the elastic modulus of the composites. We prepared samples with various volume fractions of SU-8 in the PDMS

[*] Prof. O. D. Velev, Dr. S. T. Chang, A. B. Uçar, G. R. Swindlehurst, R. O. Bradley IV
Department of Chemical and Biomolecular Engineering
North Carolina State University
Raleigh, NC 27695-7905 (USA)
E-mail: odvelev@unity.ncsu.edu
Dr. F. J. Renk
Center for Packaging Innovation
MeadWestvaco
Raleigh, NC 27606 (USA)

DOI: 10.1002/adma.200803638

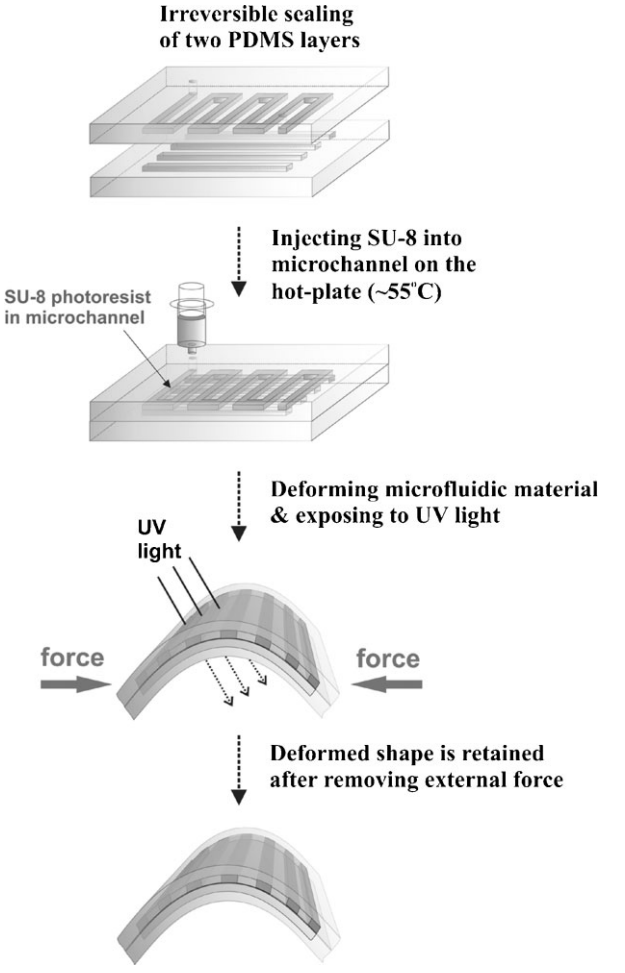

Figure 1. Fabrication of photocurable microfluidic endoskeleton structure by filling epoxy-based SU-8 photopolymer into microfluidic channel networks. During UV exposure, the SU-8 photoresist within the deformed channel network is solidified, and the preprogrammed deformation of the photocured channel network is retained, even after the external force is removed.

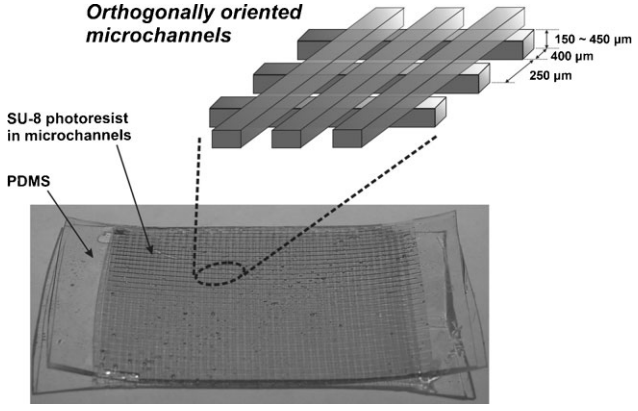

Figure 2. Orthogonally oriented microchannel structure embedded within PDMS matrix. The channel width and interchannel distance were 400 and 250 μm, respectively. The channel thickness was varied from 150 to 450 μm. The microfluidic network had an overall length of 36 mm and a width of 24 mm. The channels in the schematic are not to scale.

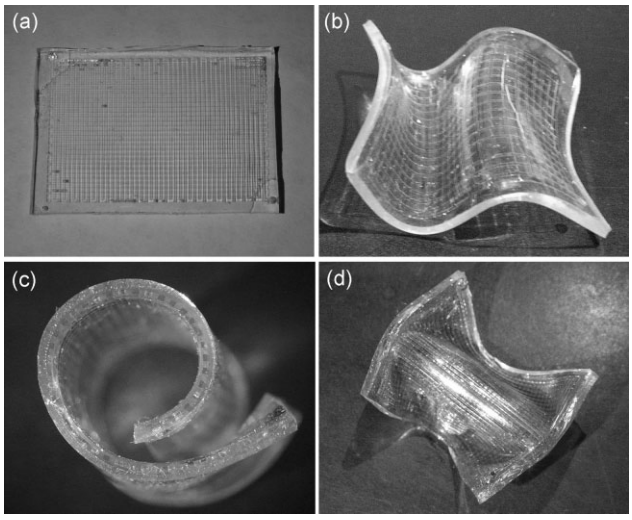

Figure 3. Photographs of PDMS sheets with embedded photocurable microfluidic endoskeleton. a) A soft and stretchable silicone sheet filled with liquid SU-8 photopolymer before UV exposure. After deforming the sheets and exposing to UV light for 15 min, the photocured microfluidic composites with solidified SU-8 photoresist retain the defined shapes, such as b) wave, c) spiral, and d) saddle. The microchannels embedded in PDMS layers were 450 μm thick in a) and d), 165 μm thick in b), and 275 μm thick in c).

matrix by changing the channel thickness, while the total thickness of the PDMS slab and other channel geometry were kept constant. Their elastic moduli were measured after photopolymerization by tension tests using a computer-controlled mechanical testing system (MTS). Typical stress–strain curves for the photocured sheets with various volume fractions of SU-8 photoresist are plotted in Figure 4a. The data demonstrate a large increase in the tensile stress of the elastomeric composite after the solidification of SU-8 in the channels. The tensile stress response of the microfluidic composites showed three regions in stress–strain relationship before complete failure, which are broadly similar to 3D woven composite materials.[37,38] The tensile stress at the initial region, called elastic phase, showed linear increase up to a strain of at least 0.6%, and was followed by a hardening phase, where a nonlinear loading response occurred. Rupture of the solidified SU-8 photoresist in the microchannels parallel to the load direction between the orthogonal channel junctions led to the primary load drop at 5–10% strain. After the sudden large load reduction, the composites with the broken SU-8 network experienced large strain displacements until the complete break at the orthogonal channel junctions. These large displacements were occurring through stretching of the elastic PDMS matrix around the failed SU-8 photoresist in the microchannel network. Although there was a variation of tensile strength and failure strain within the samples, the main characteristics of the stress–strain curves were consistent for all SU-8 endoskeleton structures.

The elastic moduli of the photocured microfluidic composites were obtained from the slopes of initial elastic regime in the stress–strain curves, and compared with the moduli of PDMS-only and noncured materials (Fig. 4b). The microchannel structures filled with liquid SU-8 had elastic moduli similar to the

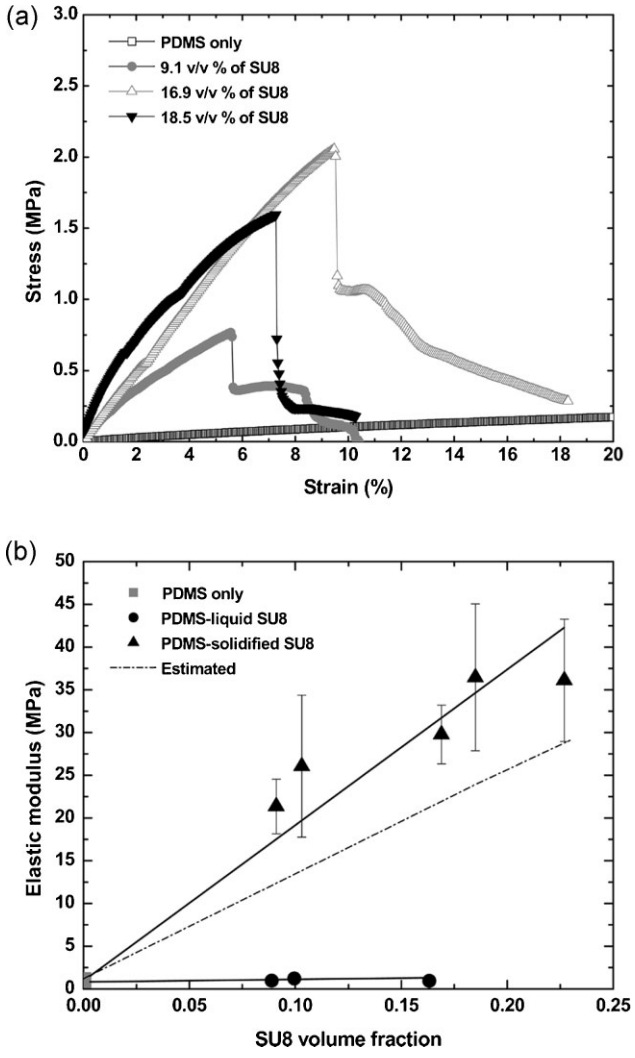

Figure 4. a) Typical stress–strain curves from tensile tests for PDMS only and photocured microfluidic endoskeleton structures containing different volume fractions of SU-8 photoresist in microchannels. b) Elastic modulus of PDMS-only layer and photocurable microfluidic networks before and after UV exposure as a function of volume fraction of SU-8 photoresist in PDMS matrix. The modulus of elasticity was obtained from the initial linear region of the stress–strain curves in a). The solid lines are least square fits. The dot-dash line is based on the estimated values by using Equation 3.

pure PDMS slabs. However, the solidification of SU-8 prepolymer in the microchannel network enhanced dramatically the elastic modulus of the microfluidic composite material, showing linear increment of the modulus with a volume fraction of SU-8 in the PDMS layers–about 40 times higher than that of the pure PDMS layer at about 20% volume of SU-8 photoresist.

The mechanical tensile properties of the sheets with photocured endoskeleton networks can be approximated as a unidirectional composite material, because the solidified photoresist bars in the microchannels are uniform in cross-section, parallel, and continuous throughout the PDMS matrix. The modulus of elasticity of unidirectional composite materials can be evaluated by rule of mixtures equations accounting for the elastic modulus and volume fraction of each component in the composite. The unidirectional composite shows different tensile behaviors depending on the orientation of the stiffer materials in the matrix with regards to the tensile loading direction. When the stiffer material components are aligned in parallel to the loading direction, the mechanical properties of the composite are described by the longitudinal tensile modulus (E_{CL}). The resistance to stretching in the direction perpendicular to the stiffer network is given by the transverse tensile modulus (E_{CT}),[39]

$$E_{CL} = \sum_{i=1}^{n} E_i V_i \tag{1}$$

$$E_{CT} = \frac{1}{\sum_{i=1}^{n} (V_i / E_i)} \tag{2}$$

where E_i and V_i are the elastic modulus and the volume fraction of component i in the composite. During the tensile loading, the elastic modulus (E_C) of the photocured microfluidic material is influenced by both longitudinal and transverse elastic moduli, due to the orthogonal microchannel structure in the PDMS matrix (Fig. 2). E_C can be estimated by[37,38]

$$E_C \approx f_S E_{CL} + (1 - f_S) E_{CT} \tag{3}$$

where f_S is the volume fraction of the solidified SU-8 photoresist that is aligned to the loading direction. As the microchannels in the top and bottom PDMS halves have the same volume, $f_S = 0.5$. The elastic moduli of solidified SU-8 photoresist without soft or post bakes and PDMS layer were measured to be ~205 and 1.2 MPa, respectively. After inserting these values in Equations 1–3, the elastic modulus of the photocured microfluidic material was calculated and plotted as a function of the volume fraction of SU-8 in Figure 4b. This estimate of the elastic modulus is in reasonable agreement with the modulus measured in the elastic regime, although the calculated value is slightly lower than the experimentally measured one. This difference might come from the additional contribution of the solidified material at the junctions and the sides of the microchannel networks to the elastic modulus. The rigidity of the SU-8 skeleton might be increased further by post-baking or over-exposure, but this is likely to lead to some brittleness of the slabs.

Overall, the results demonstrate that the solidification of SU-8 photoresist within the channel network drastically improves the stiffness of the elastomeric microfluidic materials, and the mechanical properties are approximated well by the common tensile stress equations for composite materials.

The preservation of the shape attained during photocuring is a result not only of the increased stiffness during stretching, but also the increased resistance to bending. The modulus of bending elasticity of the sheets with photocured network was measured by a Tinius-Olsen stiffness tester. Typical load-angular deflection curves of the photocured microfluidic materials with various amounts of SU-8 photoresist in the PDMS matrix are shown in

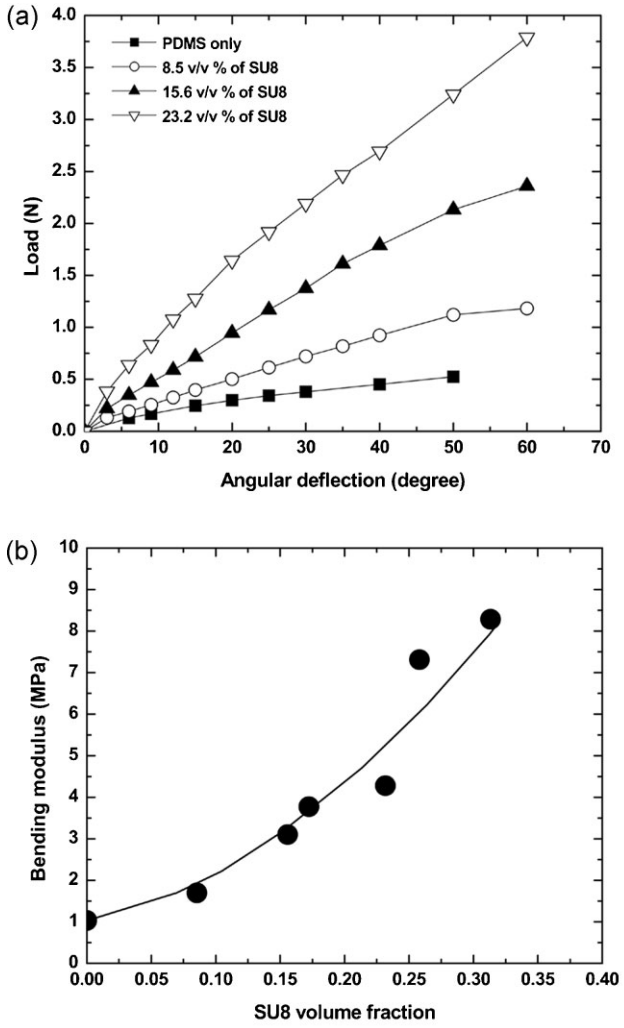

Figure 5. a) Load-angular deflection curves in bending tests for PDMS-only layer and photocured microfluidic endoskeleton structures containing different amounts of SU-8 photoresist in microchannels. b) Bending modulus of PDMS-only layer and photocurable microfluidic networks after UV exposure as a function of the volume fraction of photoresist in the matrix. The bending modulus was obtained from the initial linear region of load-angular deflection curves in a) using Equation 4. The line in b) is a guide to the eye.

Figure 5a. In order to produce the same angular deflection, higher force had to be applied to the microfluidic materials with larger amounts of the solidified SU-8 photoresist. The bending modulus (E_B) of the photocurable microfluidic structure was calculated from the slope (m) of the initial straight line of the moment-angular deflection curve according to[40,41]

$$E_B = \frac{4Sm}{wd^3} \quad (4)$$

where S is the span length measured from the center of rotation of the pendulum weighing system to the contact edge of the bending plate, and w and d are the width and depth of test sample, respectively.

Similarly to the tensile tests, the bending modulus of the photocured endoskeleton structure increased up to one order of magnitude with the increase in the volume fraction of SU-8 photoresist in the PDMS layer (Fig. 5b). The material became harder to bend and immediately recovered the memorized shape after unloading. The bending failure force of the photocured microfluidic materials was not measured because most samples did not break under the loading conditions in this measurement. This remarkable flexibility of the material might arise from the enclosing of the rigid polymer shell in the elastic sheath, but the effect was not quantified. Clearly, the network of solidified SU-8 photoresist imparts high rigidity to the elastomeric silicone matrix and renders possible the recovery of the programmed shapes with highly recoverable strain. The mechanical strength of the photocured polymer-endoskeleton network could be drastically improved with the introduction of truss or other 3D microchannel structures in the PDMS matrix or by adding microfibers to the photopolymer filling in the microchannels.

In summary, we demonstrate that the light-triggered solidification of SU-8 photoresist in the microfluidic endoskeleton of normally flexible PDMS layers leads to shape preservation with high strain storage and recovery. The permanent locking in of the shape of light-solidified microfluidic sheets could be used in fabricating instant containers, patches, and supports on demand, creating "exoskeletons" for delicate package contents, rapid prototyping, and multiple other applications. Microfluidic devices containing both regular and SU-8-filled channels might be dynamically reconfigured by UV exposure. The fabrication process of the materials with microfluidic endoskeleton that we report here could be simple and scalable. The photocurable polymer precursor inside the microchannel network can be replaced with other shape-memory materials, which can retain shape and develop strain when actuated by external stimuli such as heat and electric or magnetic fields.

Experimental

Channel masters were created by coating SU-8 2050 photoresist (MicroChem, Inc.) on a silicon wafer to a thickness from 150 to 450 μm using a spin-coater (Model P6700, Specialty Coating Systems, Inc.). The transparency photomasks containing channel designs with a 400 μm of channel width were brought into contact with the SU-8 photoresist followed by UV exposure (Model B-100A, Black-Ray). After post-baking, the UV-exposed wafers were treated in SU-8 developer solution (MicroChem, Inc.) and hard-baked. The remaining steps for fabricating the shape-controlled microchannel materials are shown in Figure 1. The PDMS precursor (Sylgard 184, Dow Corning) was cast on the channel masters and cured at 70 °C. After peeling off the PDMS layers, two holes were punched at each end of the channel using a blunt 16-gauge needle to inject the photocurable polymers. Two PDMS layers with embedded channels were sealed to each other with orthogonal orientation of the channels using air-plasma treatment (Model PDC-32G, Harrick Plasma). Liquid SU-8 50 photoresist (MicroChem, Inc.) was injected into the microchannel on a hot plate (55 °C) using a syringe. The holes punched in the replicas were closed with PDMS prepolymer and cured at 70 °C. The resulting microfluidic networks had a length of 36 mm, a width of 24 mm, and a height of 1.6–2.0 mm. The photocurable microfluidic materials were deformed into a variety of shapes and exposed to UV light for 15 min to solidify the liquid SU-8 photoresist inside the microchannel networks.

For a tensile test, the microfluidic materials were cured under UV exposure for 15 min without deformation. The tensile tests were performed using an MTS tensile tester (Model MTS 30G). The crosshead speed was 25 mm min^{-1}. Tinius Olsen Stiffness tester (Tinius Olsen, Inc.) was used for measurements of the bending modulus of the sheets. One end of the photocured slabs was attached to the sample holder. A controlled load was applied steadily by a motor drive at the other free end of the samples. The applied load and the resulting angle of bending were measured from circular scales in the tester.

Acknowledgements

The authors acknowledge the support of this study from MeadWestvaco Corporation. We thank Y.-J. Choi and Dr. T.-J. Mark Luo for access to the plasma cleaner for microchannel fabrication. We are grateful to A. Krishnan, Dr. T. K. Ghosh, and Dr. J. E. Pegram for access to MTS tensile tester and Tinius-Olsen Stiffness tester. The authors also thank Dr. S. Kim for helpful discussions.

Received: December 10, 2008
Revised: February 25, 2009
Published online: April 1, 2009

[1] T. M. Squires, S. R. Quake, *Rev. Mod. Phys.* **2005**, *77*, 977.
[2] G. M. Whitesides, A. D. Stroock, *Phys. Today* **2001**, *54*, 42.
[3] G. M. Whitesides, *Nature* **2006**, *442*, 368.
[4] A. J. deMello, *Nature* **2006**, *442*, 394.
[5] S. T. Chang, E. Beaumont, D. N. Petsev, O. D. Velev, *Lab Chip* **2008**, *8*, 117.
[6] G. H. W. Sanders, A. Manz, *Trends Anal. Chem.* **2000**, *19*, 364.
[7] E. Delamarche, D. Juncker, H. Schmid, *Adv. Mater.* **2005**, *17*, 2911.
[8] J. El-Ali, P. K. Sorger, K. F. Jensen, *Nature* **2006**, *442*, 403.
[9] K. A. Shaikh, K. S. Ryu, E. D. Goluch, J.-M. Nam, J. Liu, C. S. Thaxton, T. N. Chiesl, A. E. Barron, Y. Lu, C. A. Mirkin, C. Liu, *Proc. Natl. Acad. Sci. U. S. A.* **2005**, *102*, 9745.
[10] E. A. Ottesen, J. W. Hong, S. R. Quake, J. R. Leadbetter, *Science* **2006**, *314*, 1464.
[11] H. Song, J. D. Tice, R. F. Ismagilov, *Angew. Chem. Int. Ed.* **2003**, *42*, 768.
[12] J. Kobayashi, Y. Mori, K. Okamoto, R. Akiyama, M. Ueno, T. Kitamori, S. Kobayashi, *Science* **2004**, *304*, 1305.
[13] E. R. Murphy, J. R. Martinelli, N. Zaborenko, S. L. Buchwald, K. F. Jensen, *Angew. Chem. Int. Ed.* **2007**, *46*, 1734.
[14] J. R. Millman, K. H. Bhatt, B. G. Prevo, O. D. Velev, *Nat. Mater.* **2004**, *4*, 98.
[15] D. Dendukuri, D. C. Pregibon, J. Collins, T. A. Hatton, P. S. Doyle, *Nat. Mater.* **2006**, *5*, 365.
[16] Z. Nie, W. Li, M. Seo, S. Xu, E. Kumacheva, *J. Am. Chem. Soc.* **2006**, *128*, 9408.
[17] D. Lee, D. A. Weitz, *Adv. Mater.* **2008**, *20*, 3498.
[18] R. Karnik, F. Gu, P. Basto, C. Cannizzaro, L. Dean, W. Kyei-Manu, R. Langer, O. C. Farokhzad, *Nano Lett.* **2008**, *8*, 2906.
[19] D. B. Wolfe, R. S. Conroy, P. Garstecki, B. T. Mayers, M. A. Fischbach, K. E. Paul, M. Prentiss, G. M. Whitesides, *Proc. Natl. Acad. Sci. U. S. A.* **2004**, *101*, 12434.
[20] D. V. Vezenov, B. T. Mayers, R. S. Conroy, G. M. Whitesides, P. T. Snee, Y. Chan, D. G. Nocera, M. G. Bawendi, *J. Am. Chem. Soc.* **2005**, *127*, 8952.
[21] D. Psaltis, S. R. Quake, C. Yang, *Nature* **2006**, *442*, 381.
[22] J.-M. Lim, S.-H. Kim, J.-H. Choi, S.-M. Yang, *Lab Chip* **2008**, *8*, 1580.
[23] M. J. Fuerstman, P. Garstecki, G. M. Whitesides, *Science* **2007**, *315*, 828.
[24] M. Prakash, N. Gershenfeld, *Science* **2007**, *315*, 832.
[25] S. Kim, H. N. Lee, D. van Noort, K. M. K. Swamy, S. H. Kim, J. H. Soh, K.-M. Lee, S.-W. Nam, J. Yoon, S. Park, *Angew. Chem. Int. Ed.* **2008**, *47*, 872.
[26] R. A. Hayes, B. J. Feenstra, *Nature* **2003**, *425*, 383.
[27] A. C. Siegel, D. A. Bruzewicz, D. B. Weibel, G. M. Whitesides, *Adv. Mater.* **2007**, *19*, 727.
[28] M. K. S. Verma, A. Majumder, A. Ghatak, *Langmuir* **2006**, *22*, 10291.
[29] A. Majumder, A. Ghatak, A. Sharma, *Science* **2007**, *318*, 258.
[30] K. S. Toohey, N. R. Sottos, J. A. Lewis, J. S. Moore, S. R. White, *Nat. Mater.* **2007**, *6*, 581.
[31] D. C. Duffy, J. C. McDonald, O. J. A. Schueller, G. M. Whitesides, *Anal. Chem.* **1998**, *70*, 4974.
[32] J. C. McDonald, D. C. Duffy, J. R. Anderson, D. T. Chiu, H. Wu, O. J. A. Schueller, G. M. Whitesides, *Electrophoresis* **2000**, *21*, 27.
[33] A. Govindaraju, A. Chakraborty, C. Luo, *J. Micromech. Microeng.* **2005**, *15*, 1303.
[34] H. Lorenz, M. Despont, N. Fahrni, N. LaBianca, P. Renaud, P. Vettiger, *J. Micromech. Microeng.* **1997**, *7*, 121.
[35] H. Gao, Z. Liu, G. Zhang, G. Xie, *Appl. Phys. Lett.* **2007**, *90*, 123115.
[36] R. Feng, R. J. Farris, *J. Micromech. Microeng.* **2003**, *13*, 80.
[37] B. N. Cox, M. S. Dadkhah, W. L. Morris, *Compos. Part A* **1996**, *27A*, 447.
[38] P. J. Callus, A. P. Mouritz, M. K. Bannister, K. H. Leong, *Compos. Part A* **1999**, *30*, 1277.
[39] B. D. Agarwal, L. J. Broutman, in *Analysis and Performance of Fiber Composites*, 2nd Edn., John Wiley & Sons, New York **1990**, pp. 54–120.
[40] Manual of Tinius-Olsen Stiffness tester, Tinius Olsen, Inc.
[41] W. A. Brantley, W. S. Augat, C. L. Myers, R. V. Winders, *J. Dent. Res.* **1978**, *57*, 609.